

Does bromodomain flexibility influence histone  
recognition?

## **SUPPLEMENTARY MATERIAL**

S. Steiner<sup>a</sup>, A. Magno<sup>a</sup>, D. Huang<sup>a</sup>, and A. Caffisch<sup>a\*</sup>

<sup>a</sup>Department of Biochemistry  
University of Zürich, Winterthurerstrasse 190  
CH-8057 Zürich, Switzerland  
Phone: (+41 44) 635 55 21, FAX: (+41 44) 635 68 62  
email: [caffisch@bioc.uzh.ch](mailto:caffisch@bioc.uzh.ch)

\*Corresponding author

keywords: molecular dynamics, post-translational modifications, histones,  
epigenetic targets

May 9, 2013

### Simulation systems

Bromodomain	Family	PDB entry	Number of independent runs	Total sampling ( $\mu$ s)	Number of available X-ray/NMR structures
CECR2	I	3NXB	1	0.5	1
FALZ	I	3UV2	1	0.5	2
GCN5L2	I	3D7C	1	0.5	2
PCAF	I	3GG3	1	0.5	2
BRD4(1)	II	2OSS	1	0.5	1
BRDT(1)	II	2RFJ	1	0.5	1
BRD3(2)	II	2OO1	1	0.5	2
PHIP(2)	III	3MB3	1	0.5	1
WDR9(2)	III	3Q2E	1	0.5	1
<b>CREBBP</b>	III	3DWY	5	<b>4.5</b>	1
EP300	III	3I3J	1	0.5	1
ATAD2	IV	3DAI	1	0.5	1
<b>BRD1</b>	IV	3RCW	5	<b>4.5</b>	1
<b>BAZ2B</b>	V	3G0L	5	<b>4.5</b>	1
TAF1(1)	VII	3UV5	1	0.5	2
TAF1L(2)	VII	3HMH	1	0.5	1
<b>TAF1(2)</b>	VII	3UV4	4	<b>4.0</b>	2
ASH1L	VIII	3MQM	1	0.5	1
PB1(2)	VIII	3HMF	1	0.5	1
SMARCA4	VIII	3UVD	1	0.5	3

Table S-I: The digit in parentheses in the first column indicates the position of the bromodomain along the polypeptide sequence, e.g., TAF1(2) is the second bromodomain of the human Transcription initiation factor TFIID subunit 1 (TAF1). Multiple independent MD runs were carried out for the four bromodomains in boldface. The family classification and number of available X-ray/NMR structures are taken from Ref.<sup>1</sup>

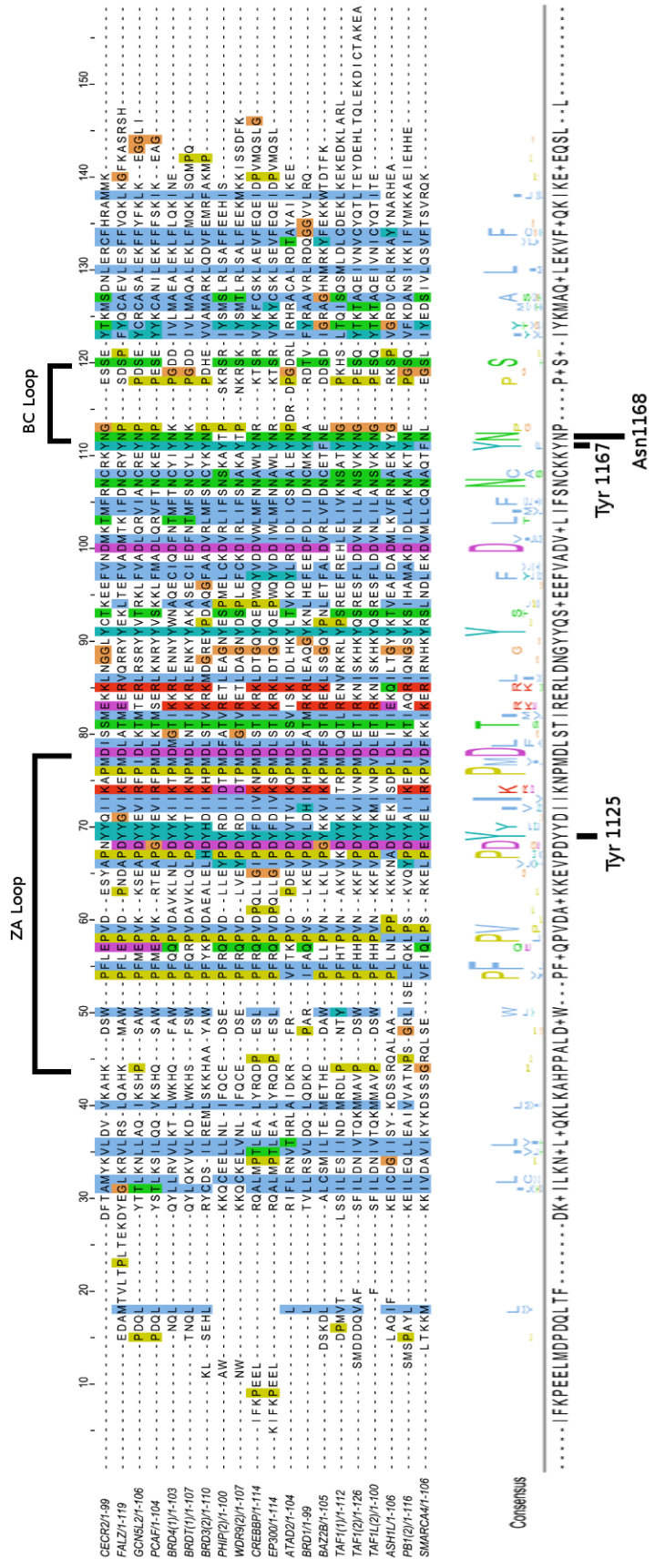


Figure S1: **Sequence alignment of the 20 simulated bromodomains.** The sequences were aligned first with MUSCLE<sup>2</sup> and subsequently realigned with ClustalW<sup>3</sup> using default setting parameters. Residues are colored following the ClustalX color scheme. The three residues in the bottom emphasize the evolutionary conserved Tyr side chain on the ZA-loop, i.e., Tyr1125 in CREBBP, Tyr599 in BRD1, Tyr1901 in BAZ2B, and Tyr1561 in TAF1(2), and the conserved aromatic residue and Asn at the beginning of the BC-loop, i.e., Tyr1167-Asn1168 in CREBBP, Tyr641-Asn642 in BRD1, Phe1943-Asn1944 in BAZ2B, and Tyr1603-Asn1604 in TAF1(2). The conserved residues are labeled only for CREBBP.

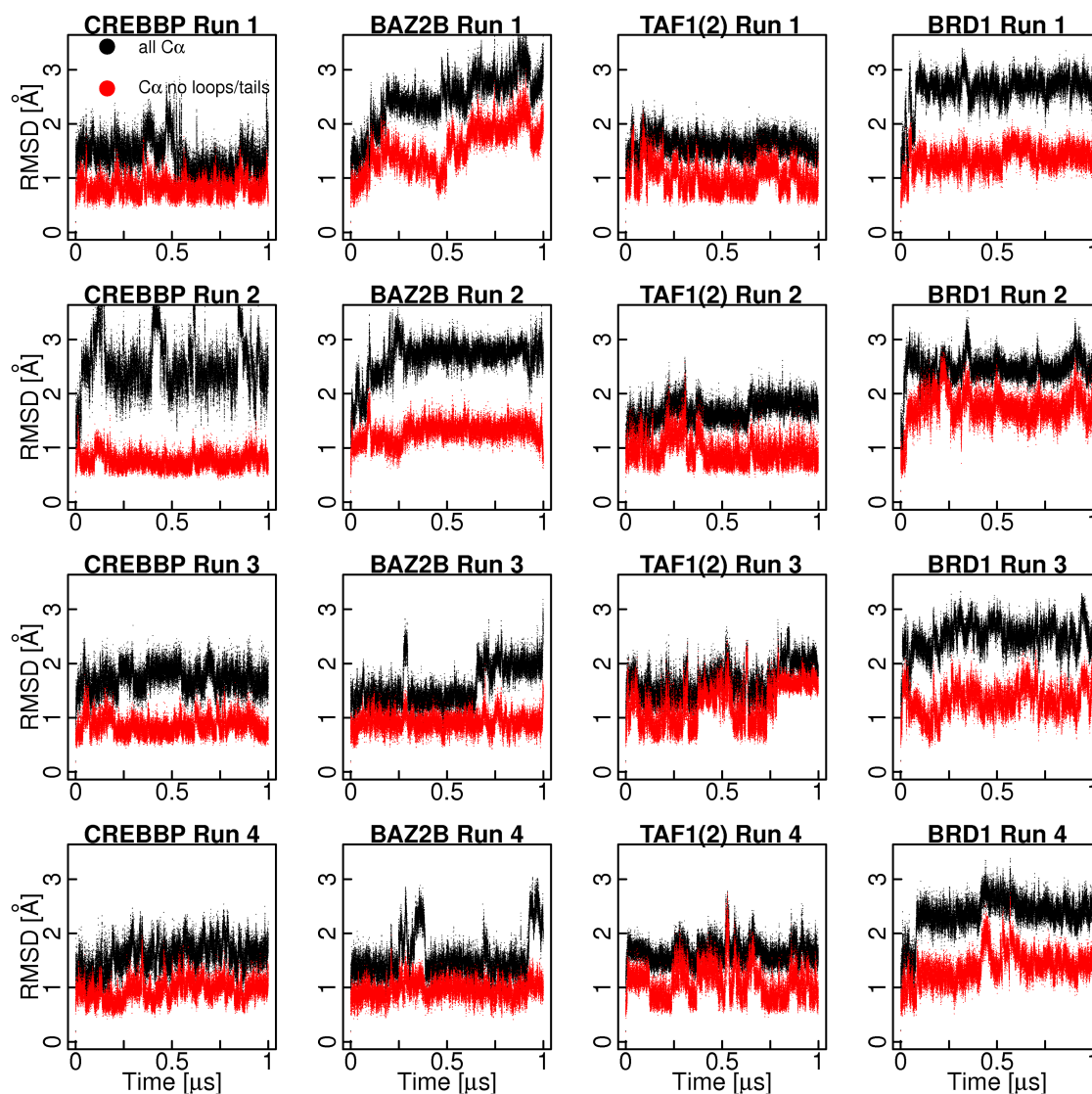


Figure S2: **Root mean square deviation (RMSD) of C $\alpha$  atoms.** The time series of the RMSD from the minimized structures (i.e., starting structure of the MD runs) is plotted for all C $\alpha$  atoms (black line) and excluding the C $\alpha$  atoms in the ZA-loop, BC-loop, and the termini (red line). For CREBBP C $\alpha$ 's of residues 1104-1134 and 1168-1172 as well as 3 terminal residues on each N- and C-terminus were excluded for the latter calculation. For BAZ2B, BRD1 and TAF1(2) the corresponding residues upon structural overlap were neglected. Note that similar RMSD values are observed for the other 16 bromodomains.

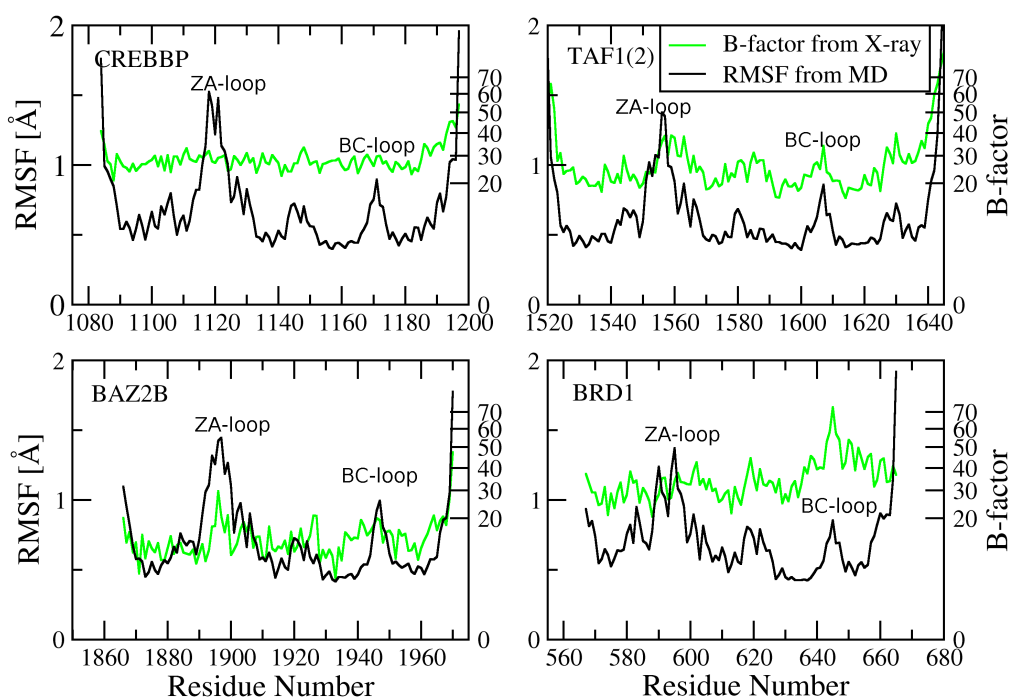


Figure S3: **Root mean square fluctuations (RMSF)**. Profile of the RMSF of the  $C_{\alpha}$  atoms (black line,  $y$ -axis on the left) of CREBBP, BAZ2B, BRD1 and TAF1(2) and crystallographic B-factors (green line,  $y$ -axis on the right) as a function of residue number. The RMSF values were averaged over simulation intervals of 5 ns. The fluctuations are highest for the ZA-loop, BC-loop, and termini. Note that the major discrepancies between RMSF along the simulations and crystallographic B-factors are due to crystal contacts in the latter, e.g., for the loops of CREBBP which are stabilized by the nearest neighbors in the crystal (PDB code 3DWY).

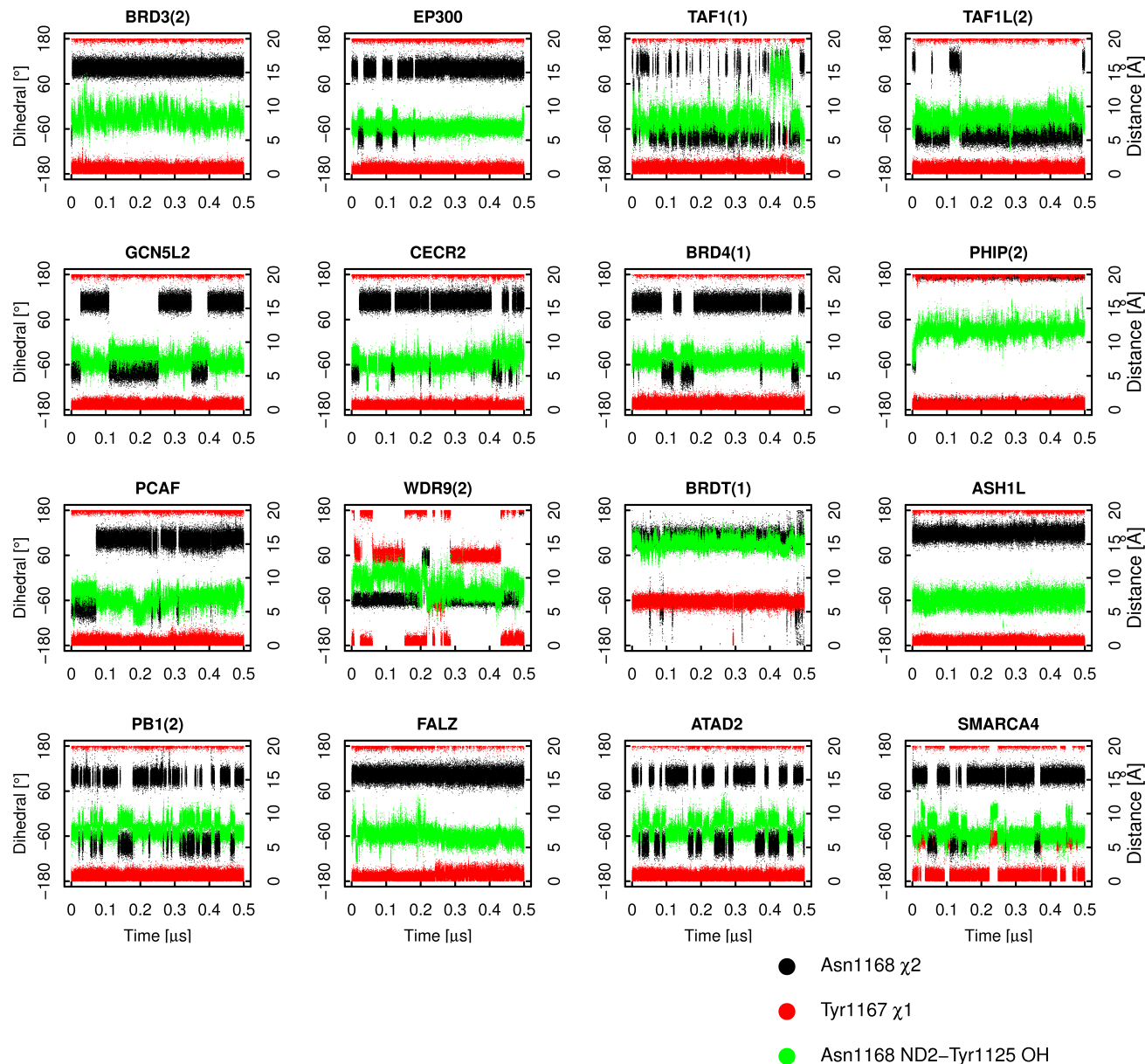


Figure S4: **Conserved Asn and Tyr/Phe: Time series of dihedrals and distances.** The  $\chi_2$  dihedral of the conserved Asn (i.e., Asn1168 of CREBBP) is shown (black). Note that for PHIP(2) and WDR9(2)  $\chi_1$  of Thr equivalent to Asn1168, and for ASH1L  $\chi_2$  of Tyr equivalent to Asn1168 are shown. The  $\chi_1$  of Tyr/Phe preceding in sequence the conserved Asn (i.e., Tyr1167 in CREBBP) is also shown (red). The distance between the side chain ND2 of the conserved Asn and the hydroxyl oxygen of the ZA-loop Tyr pointing inside the binding groove (i.e., Tyr1125 in CREBBP) is also shown (green); in case of a Thr or Tyr in position of the conserved Asn, Thr OG1, resp. Tyr OH were used instead of Asn ND2. Note that the ZA-loop Tyr is conserved in all the 20 bromodomains investigated here (see Figure S1).

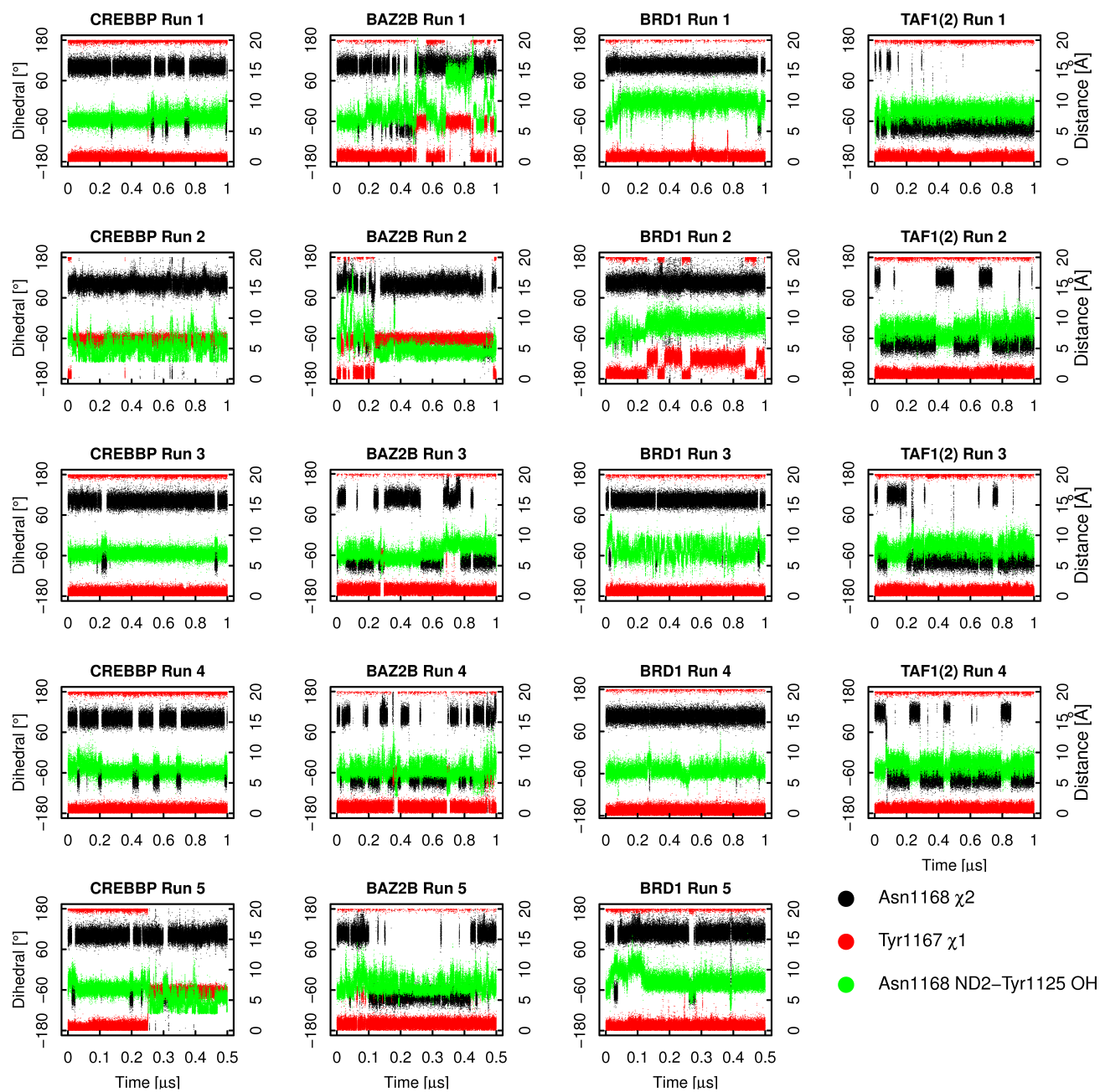


Figure S5: **Conserved Asn and Tyr/Phe: Time series of dihedrals and distances.** Same as Figure S4 for the four bromodomains for which multiple MD simulations were carried out.

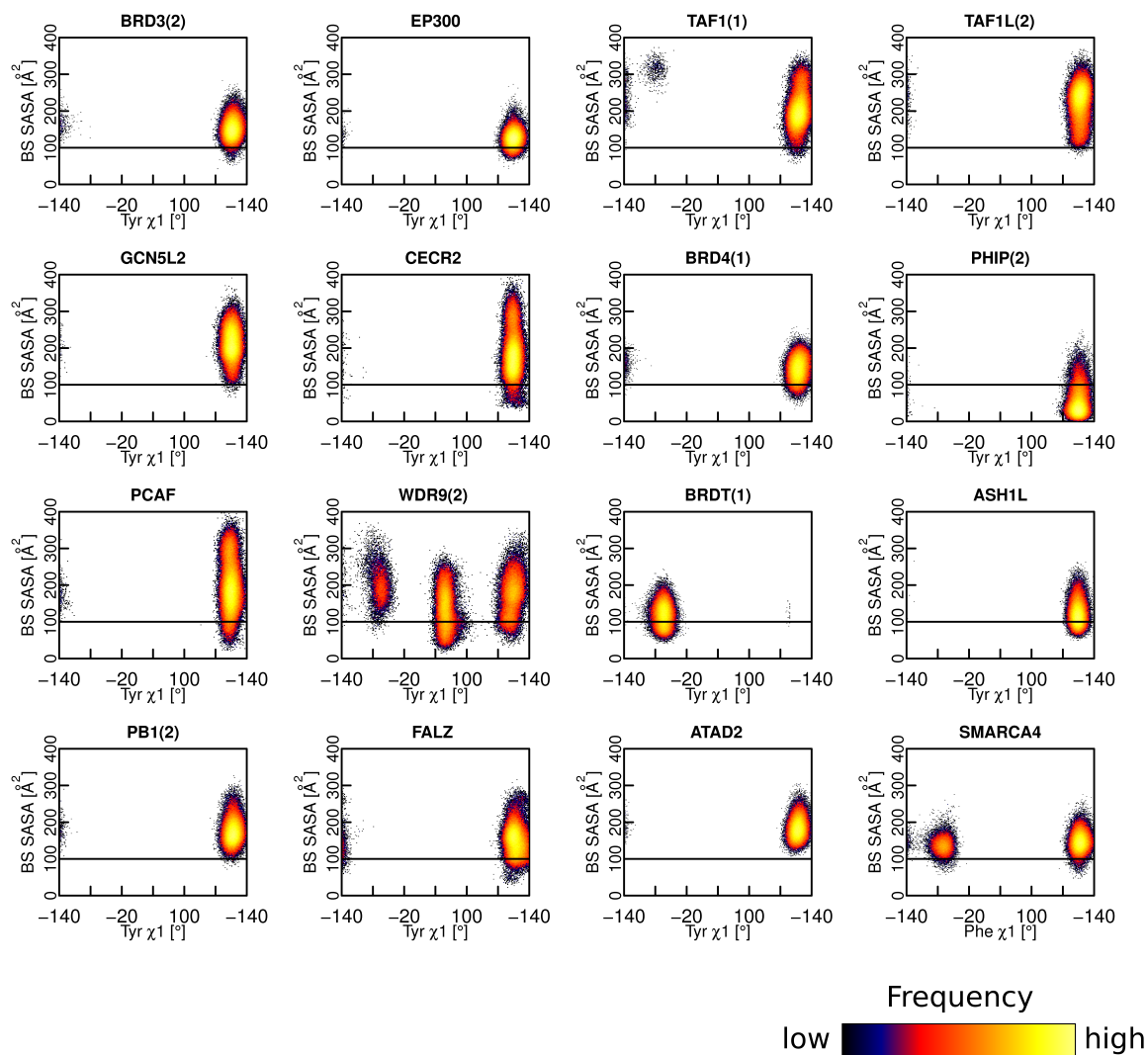


Figure S6: **Binding site accessible surface.** Two-dimensional histograms of binding site accessible molecular surface (SASA) versus  $\chi_1$  dihedral of Tyr/Phe preceding the conserved Asn in the BC-loop. Coloring according to frequencies follows a logarithmic scale.



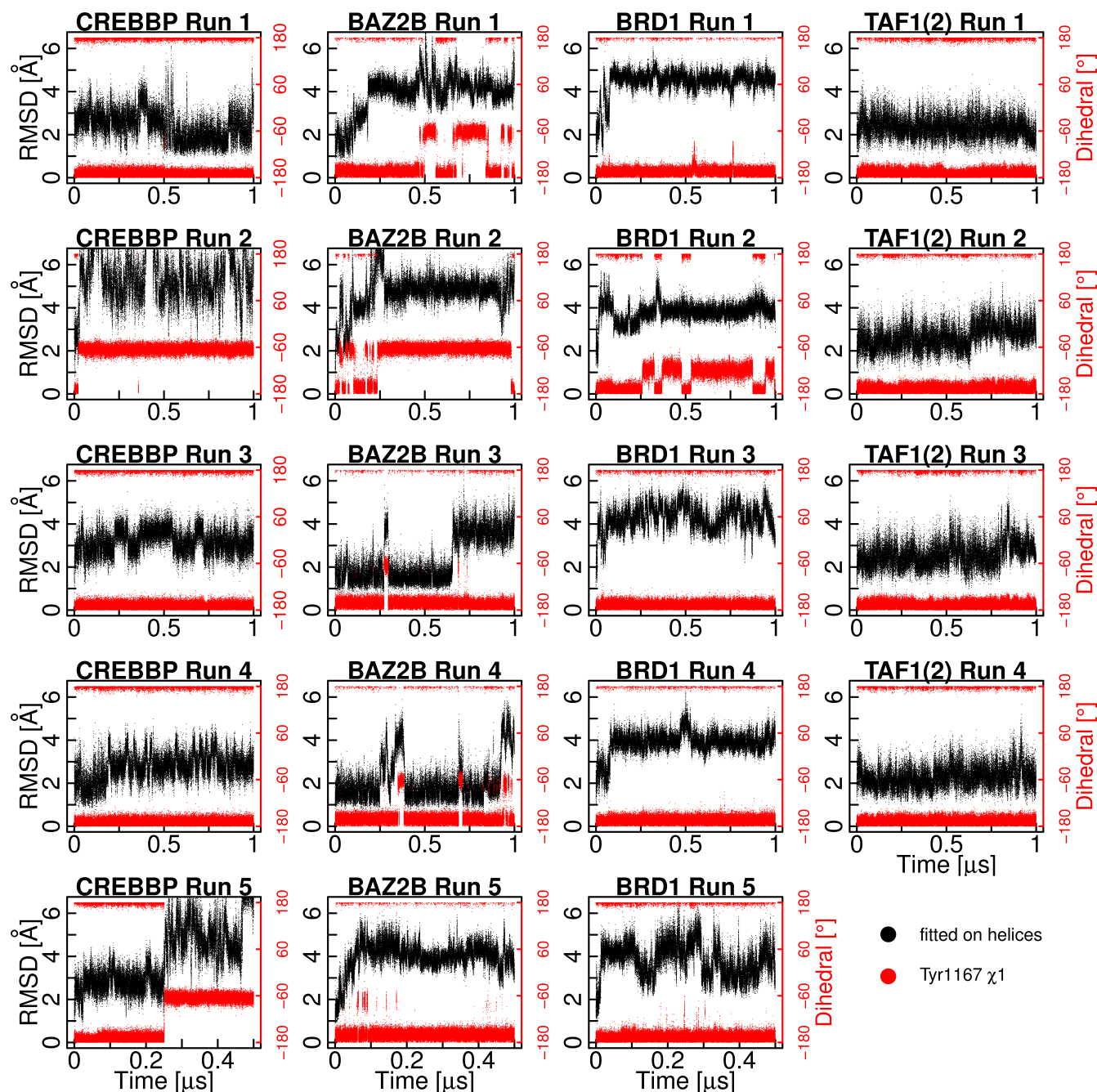


Figure S7: **Flexibility of ZA-loop and side chain rotation of the conserved Tyr/Phe in BC-loop.** Each panel corresponds to an independent simulation (of the bromodomain indicated in the top) and shows the time series of RMSD of the  $C_\alpha$  atoms of the ZA-loop (black, y-axis on the left) and the  $\chi_1$  dihedral angle of the conserved Tyr/Phe in the BC-loop (red, y-axis on the right). The RMSD of the ZA-loop from the energy-minimized crystal structure was calculated upon structural overlap of the MD snapshots using the  $C_\alpha$  atoms of the four  $\alpha$ -helices.

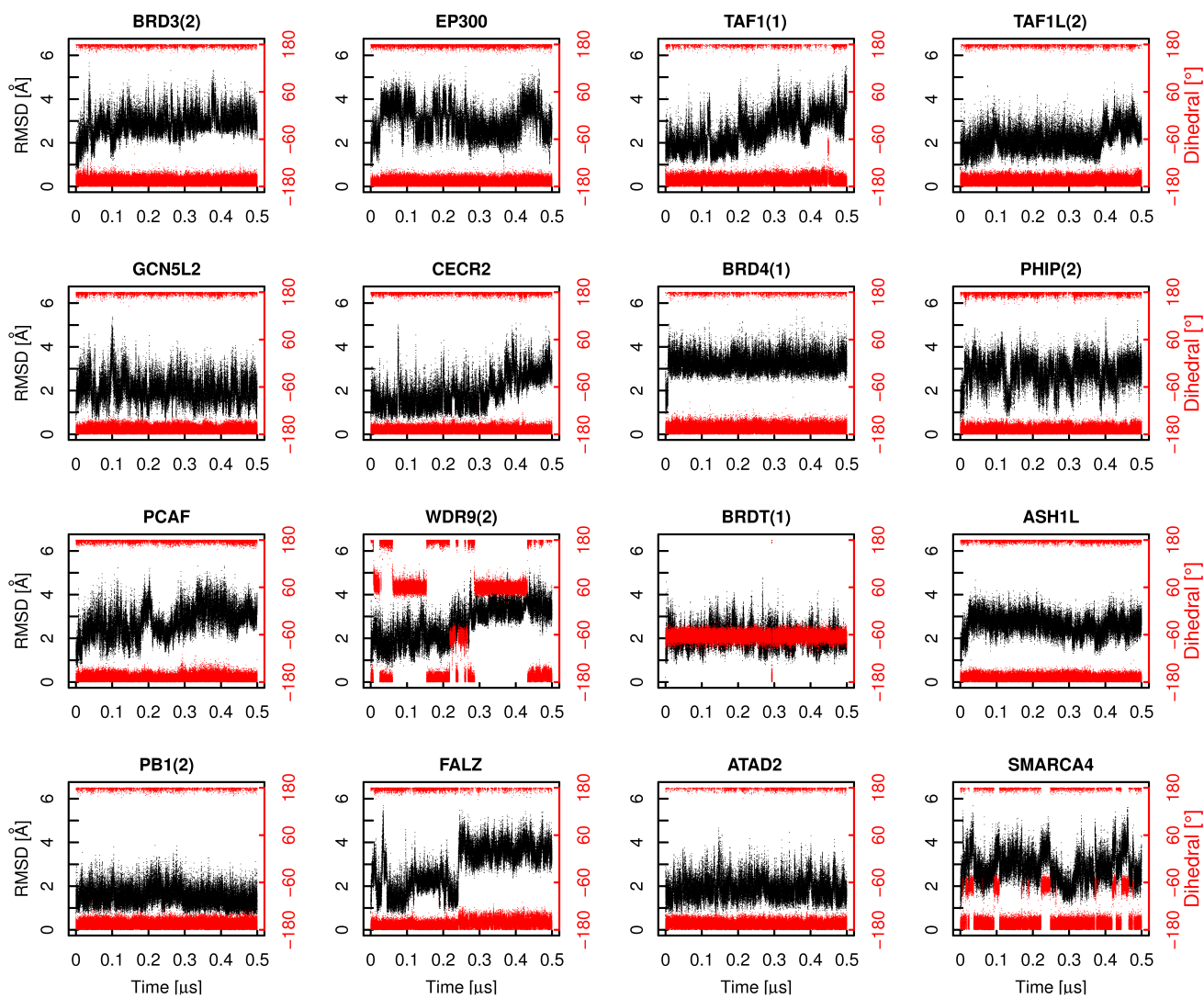


Figure S8: Flexibility of ZA-loop and side chain rotation of the conserved Tyr/Phe in BC-loop. See caption of Figure S7.

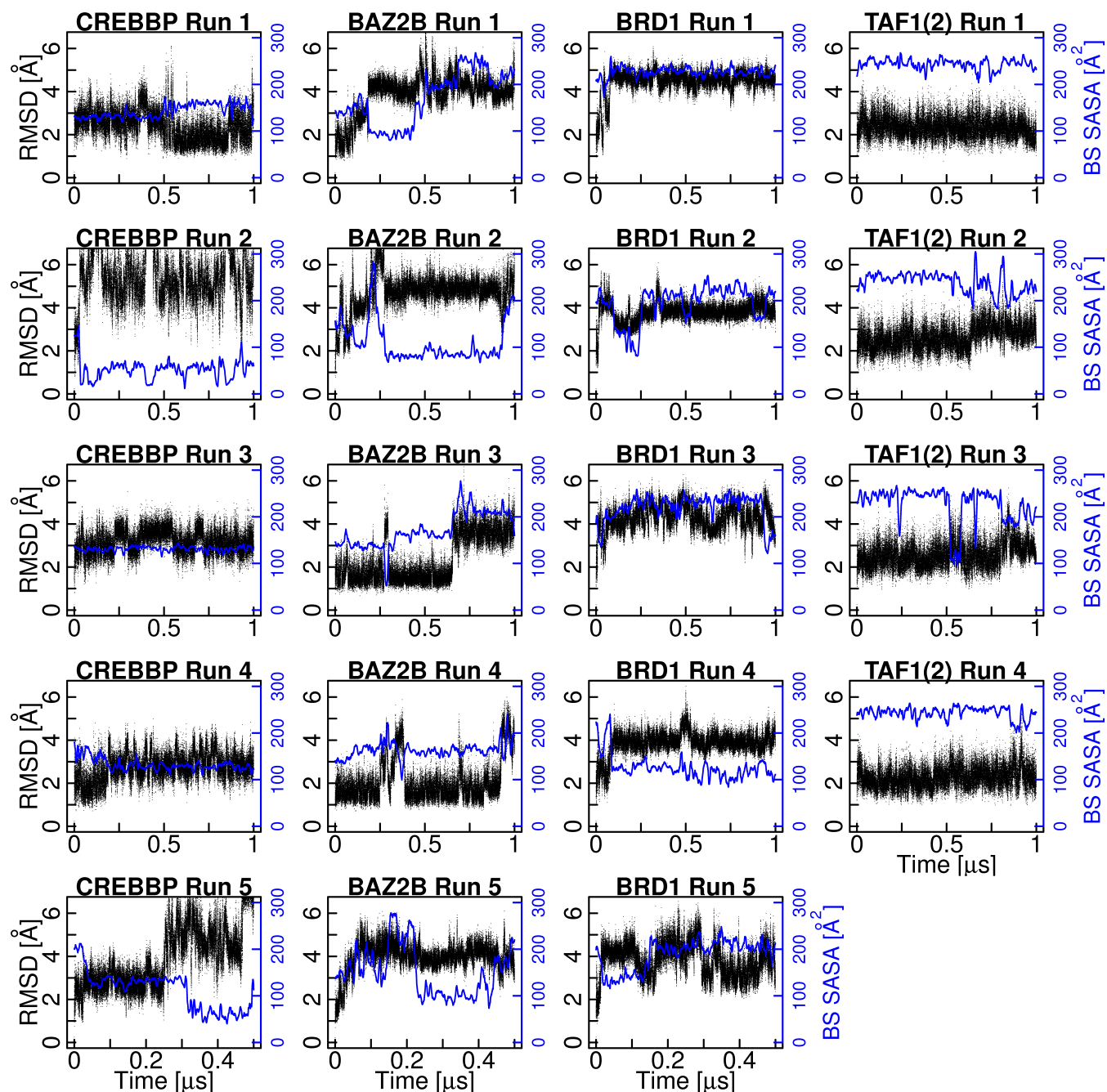


Figure S9: **Flexibility of ZA-loop and changes in binding site SASA.** Each panel corresponds to an independent simulation (of the bromodomain indicated in the top) and shows the time series of RMSD of the  $C_{\alpha}$  atoms of the ZA-loop (black, y-axis on the left) and the binding site SASA (blue, y-axis on the right, running average calculated over time intervals of 10 ns for clarity). The RMSD of the ZA-loop from the energy-minimized crystal structure was calculated upon structural overlap of the MD snapshots using the  $C_{\alpha}$  atoms of the four  $\alpha$ -helices.

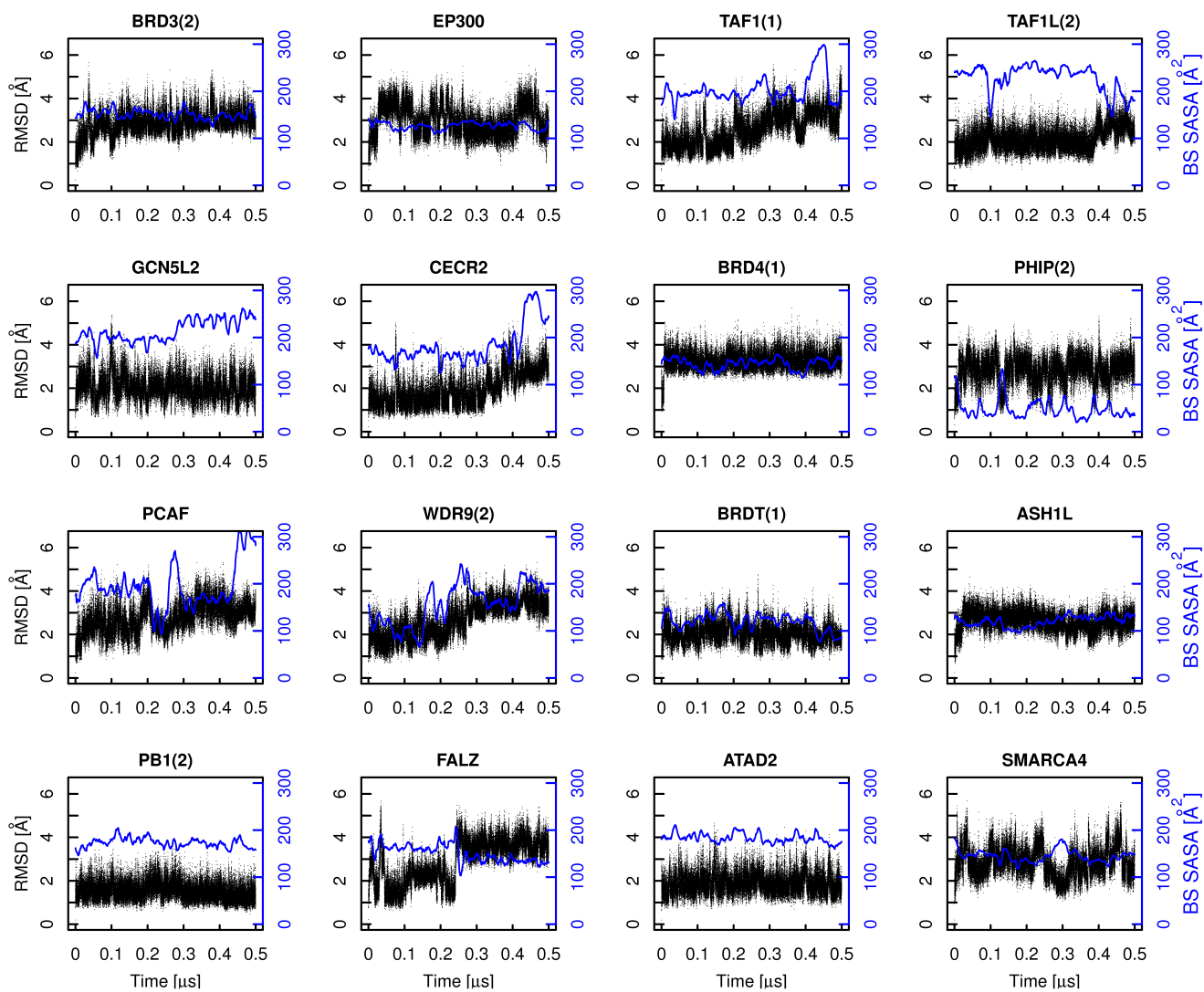


Figure S10: Flexibility of ZA-loop and changes in binding site SASA. See caption of Figure S9.

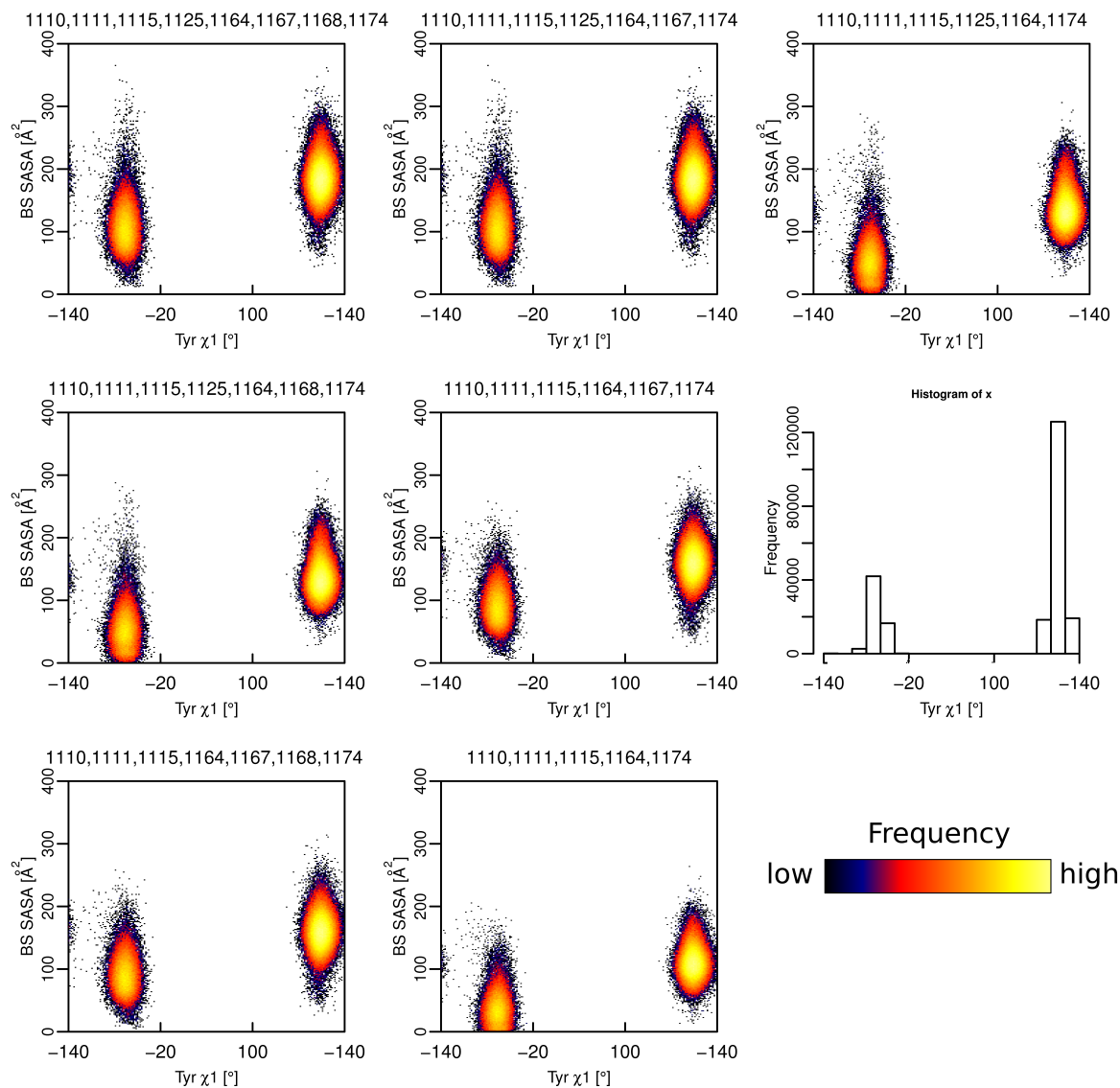


Figure S11: **Robustness of two-dimensional histograms.** The very similar two-dimensional histograms of binding site SASA vs.  $\chi_1$  of Tyr1167 for CREBBP, calculated using seven different selections of binding site atoms, demonstrate robustness. The subset of binding site residues used for each of the seven panels are the side chain heavy atoms of the residues whose numbers are mentioned above each panel. Coloring according to frequencies follows a logarithmic scale. The one-dimensional histogram of the  $\chi_1$  of CREBBP Tyr1167 is also shown (middle right).

## References

- [1] Filippakopoulos, P., Picaud, S., Mangos, M., Keates, T., Lambert, J.-P., Barsyte-Lovejoy, D., Felletar, I., Volkmer, R., Müller, S., Pawson, T., Gingras, A.-C., Arrowsmith, C. H., and Knapp, S. Histone recognition and large-scale structural analysis of the human bromodomain family. *Cell* 149(1):214–231, 2012.
- [2] Edgar, R. C. MUSCLE: multiple sequence alignment with high accuracy and high throughput. *Nucleic Acids Research* 32(5):1792–1797, 2004.
- [3] Larkin, M., Blackshields, G., Brown, N., Chenna, R., McGettigan, P., McWilliam, H., Valentin, F., Wallace, I., Wilm, A., Lopez, R., Thompson, J., Gibson, T., and Higgins, D. Clustal W and Clustal X version 2.0. *Bioinformatics* 23(21):2947–2948, 2007.